Published in final edited form as:
Biochim Biophys Acta. 2008 November ; 1778(11): 2469–2479. doi:10.1016/j.bbamem.2008.07.024.

RYANOIDS AND IMPERATOXIN AFFECT THE MODULATION OF CARDIAC RYANODINE RECEPTORS BY DIHYDROPYRIDINE RECEPTOR PEPTIDE A

Maura Porta[*,1], **Paula L. Diaz-Sylvester**[*,2], **Alma Nani**[3], **Josefina Ramos-Franco**[3], and **Julio A. Copello**[2]

[1]Department of Physiology, Loyola University Chicago, Maywood, IL

[2]Department of Pharmacology, Southern Illinois University School of Medicine, Springfield, IL

[3]Department of Molecular Biophysics and Physiology, Rush University, Chicago, IL

Abstract

Ca^{2+}-entry via L-type Ca^{2+} channels (DHPR) is known to trigger ryanodine receptor (RyR)-mediated Ca^{2+}-release from sarcoplasmic reticulum (SR). The mechanism that terminates SR Ca^{2+} release is still unknown. Previous reports showed evidence of Ca^{2+}-entry independent inhibition of Ca^{2+} sparks by DHPR in cardiomyocytes. A peptide from the DHPR loop II–III (PepA) was reported to modulate isolated RyRs. We found that PepA induced voltage-dependent "flicker block" and transition to substates of fully-activated cardiac RyRs in planar bilayers. Substates had less voltage-dependence than block and did not represent occupancy of a ryanoid site. However, ryanoids stabilized PepA-induced events while PepA increased RyR2 affinity for ryanodol, which suggests cooperative interactions. Ryanodol stabilized Imperatoxin A ($IpTx_A$) binding but when $IpTx_A$ bound first, it prevented ryanodol binding. Moreover, $IpTx_A$ and PepA excluded each other from their sites. This suggests that $IpTx_A$ generates a vestibular gate (either sterically or allosterically) that prevents access to the peptides and ryanodol binding sites. Inactivating gate moieties ("ball peptides") from K^+ and Na^+ channels (ShakerB and KIFMK, respectively) induced well resolved slow block and substates, which were sensitive to ryanoids and $IpTx_A$ and allowed, by comparison, better understanding of PepA action. The RyR2 appears to interact with PepA or ball peptides through a two-step mechanism, reminiscent of the inactivation of voltage-gated channels, which includes binding to outer (substates) and inner (block) vestibular regions in the channel conduction pathway. Our results open the possibility that "ball peptide-like" moieties in RyR2-interacting proteins could modulate SR Ca^{2+} release in cells.

INTRODUCTION

In striated muscle, ryanodine receptor channels (RyR) located at the sarcoplasmic reticulum (SR) calcium stores are the main pathway for intracellular Ca^{2+} release upon physiological or pharmacological stimulation [1], [2] and [3].

Address correspondence to: Julio A. Copello, SIU-Med, Department of Pharmacology, 801 North Rutledge Street, Room 3257, PO BOX 19629, Springfield, IL 62794-9629, E-mail: jcopello@siumed.edu.

*Both authors have contributed equally to the work.

Functional studies of gating of RyR channel molecules require their isolation from cells [4] and [5]. The response to pharmacological and physiological agonists of these isolated RyRs, studied in lipid bilayers or purified SR vesicles, is similar to that of RyR-mediated Ca^{2+} signaling in cells [3], [6] and [7]. However, the non-inactivating behavior and Ca^{2+} dependence of RyR in bilayers and microsomes cannot explain why the calcium release process in cells terminates while cytosolic and lumenal Ca^{2+} still remain at levels that suffice to keep isolated RyR channels fully active [3] and [8].

In skeletal muscle, L-type Ca^{2+} channels (DHPR) activate RyR1-mediated SR Ca^{2+} release through physical interactions [1], [2], [3] and [9]. Differently, in heart, DHPR-mediated Ca^{2+} entry is required for effective activation of cardiac RyR2 during excitation contraction coupling [1], [2], [3], [9] and [10]. Under resting conditions, however, DHPR-RyR physical interactions seem to occur in both cell types, which completely (in skeletal fibers) or partially (in cardiac myocytes) prevent Ca^{2+} sparks [9], [10], [11], [12], [13] and [14]. Various peptides from DHPR cytosolic domains modulate the function of isolated RyRs [15], [16], [17], [18], [19], [20], [21], [22], [23], [24], [25], [26], [27] and [28]. Interestingly, a peptide domain from the II–III loop of the skeletal DHPR (α subunit) named Peptide A modulates both cardiac and skeletal RyRs [25], [26], [27] and [28]. The action of Peptide A on RyRs is complex and may include activation, inhibition and the production of substates [22], [25], [26], [27] and [28].

The aim of this work was to further characterize the action of Peptide A on fully activated cardiac RyR2. Caffeine activated-RyR2s were selected as they are more appropriate to study the action of pore-blockers or substate-inducing agents and they can better mimic the gating status of RyRs upon fast activation by Ca^{2+} in cells [29] and [30]. We also determined if Peptide A-induced subconductance states represent the interaction of this peptide with binding sites in the RyR2 for two well known conductance modifiers, ryanodine and Imperatoxin A.

There is functional homology between the structure of the cytosolic conduction pathway in RyR2 and those in voltage-gated K^+ and Na^+ channels [31]. Therefore, we compare the action of Peptide A to that of peptides homolog to cytosolic regions (ball peptides) of voltage-gated K^+ and Na^+ channels known to participate in the physiological inactivation of their respective channels (Shaker B [32] and KIFMK [33], respectively). Although KIFMK is simpler and smaller than Peptide A and Shaker B, we found that the three peptides acted as voltage-dependent blockers of RyR2 and they all induced substates. The action of peptides was profoundly affected by ryanoids and by Imperatoxin A. Some of these results have been presented in preliminary form [34] and [35].

MATERIALS AND METHODS

Drugs and chemicals

$CaCl_2$ standard for calibration was from Word Precision Instruments Inc. (Sarasota, FL). Phospholipids were obtained from Avanti (Alabaster, AL). Ryanodine was from Calbiochem (San Diego, CA). Ryanodol was obtained from hydrolyzed ryanodine as previously described [36]. All other drugs and chemicals were either from Sigma-Aldrich or were reagent grade.

Peptides

Imperatoxin A ($IpTx_A$; GDCLPHLKRCKADNDCCGKKCKRRGTNAEKRCR) was from Alomone Labs (Jerusalem, Israel). Peptide A (TSAQKAKAEERKRRKMSRGL) from the skeletal DHPR II–III loop, Shaker B (MAAVAVLYVLGKKRQHRKKQ), and Na^+ channel inactivating peptide (acetyl-KIFMK-amide) were custom-synthesized and purified by Alpha Diagnostics Inc. (San Antonio, TX).

Sarcoplasmic reticulum microsomes

All procedures with animals were designed to minimize pain and suffering and conformed to the guidelines of the National Institutes of Health. The committee on the Use and Care of Laboratory Animals (LACUC) of Southern Illinois University School of Medicine reviewed and approved the protocols for animal use. Sarcoplasmic reticulum membrane fractions were obtained from rabbit skeletal muscle and dog heart ventricle using cellular subfractionation methods based on Saito et al., 1984 [37] and Chamberlain et al., 1983 [4]. After isolation, the bulk of SR preparations was aliquoted into 300 μl cryovials and kept in liquid nitrogen (better and safer long-term storage). Every month, the content of a few cryovials are aliquoted (15 μl each) and stored at −80°C for easy access. For experiments, aliquots were quickly thawed in water, kept in ice and used within 3–5 hours.

Bilayer technique

Reconstitution of RyR2 in planar lipid bilayers, was done as previously described [38]. Briefly, planar lipid bilayers were formed on 80 to 100 μm-diameter circular holes in teflon septa, separating two 1.3 ml compartments. The *trans* compartment was filled with HEPES-Ca^{2+} solution containing HEPES 250 mM and $Ca(OH)_2$ 53 mM, pH 7.4. The *trans* compartment was clamped at 0 mV using an Axopatch 200B patch-clamp amplifier (Axon Instruments, Foster City, CA). The *cis* compartment (ground) was filled with HEPES-Tris solution containing HEPES 250 mM and TrisOH 118 mM, pH 7.4. Bilayers of a 5:4:1 mixture of bovine brain phosphatidylethanolamine, phosphatidylserine and phosphatidylcholine (45–50 mg/ml in decane) were painted onto the holes of teflon septa from the *cis* side. A mixture of BAPTA and dibromo-BAPTA was used to buffer free [Ca^{2+}] on the cytosolic surface of the channel ($[Ca^{2+}]_{cyt}$) [38]. As previously done [38], RyR channels were identified by current amplitudes (~3.5 pA at 0 mV), slope conductance (~100 pS, and reversal potential ~−45 mV, *trans* - *cis*) and response to diagnostic ligands (e.g., ryanodine, Ca^{2+}, ATP, caffeine and Ruthenium Red). RyR channel currents are depicted as positive (upward deflections of the current) in figures and reflect cation flux from the *trans* (luminal) to the *cis* (cytosolic) compartment. Membrane voltages always represent the difference *trans* - *cis* compartments (in mV).

Single channel analysis

Channel currents were first filtered through the Axopatch 200B low-pass Bessel filter at 2 kHz, digitized at 20 kHz with an analog to digital converter (Digidata 1320, Axon Instruments) and stored on DVD. Recordings were analyzed using pClamp9 software (Axon Instruments). Analysis with this program included open times, closed times and open probabilities (P_o), which were determined by half-amplitude threshold analysis of single-channel recordings as done before [38].

Recordings were digitally filtered at 500 Hz (experiments at $V_m \geq 0$ mV) or 400 Hz (experiments at $V_m < 0$ mV or all V_m in presence of ryanodine) in order to estimate the probabilities of substates using two different methods:

1) Manual analysis of the traces—Frame by frame analysis (100ms/frame) was performed using pClamp9 on each 4-min recording. In most of our recordings, we were able to distinguish different levels of current that included the baseline (blocked channels), full openings and 1–3 main substate levels. Events, at different levels of current lasting more than 3 ms, were manually selected. The parameters (mean amplitude and duration) of each event were collected and averaged. The probability of substate occurrence, $P_{substate}$, was estimated from the ratio: time spent in substate/total recording time. P_{block} was estimated as the fraction of time spent in baseline current (block state).

2) Current-amplitude distributions—All-points current-amplitude histograms (band width = 0.01 pA) were obtained from each 4-min recording. Histograms were normalized so that total histogram area = 1. In most of our experiments, we were able to detect peaks (components) corresponding to the baseline, full opening and 1–3 substate levels. Each component was fitted with a Gaussian function using the Levenberg-Marquardt method. When the fitting is good, the fitted area of each component can be used as an estimation of its probability. This was the case when we analyzed the recordings shown in Fig. 2D, Fig. 3 and Fig. 7 where the current-amplitude distribution analysis and the frame by frame analysis provided statistically identical results.

In the presence of ryanodine, the probabilities of Shaker B and KIFMK -induced substates were determined using frame by frame analysis and they were only significant at $V_m \leq 0$. In the absence of ryanodine, KIFMK-induced substates are rare and do not significantly affect the current-amplitude distribution. In the presence of ryanodine at $V_m < 0$, the small signal-to-noise ratio precluded the unequivocal resolution of all individual components from the amplitude distribution histograms. In these cases, the $P_{substate}$ were only estimated using frame by frame analysis.

In the presence of Peptide A, the probability of ryanodol-induced substates was also estimated using frame by frame analysis. The length of ryanodol-induced events (ranging 0.1–1 sec) allowed excellent resolution despite the occurrence of Peptide A-induced block and substates. Similarly, the probabilities of $IpTx_A$-induced substates (ranging 0.1–1 sec) in the presence of Peptide A, Shaker B or KIFMK were determined using frame by frame analysis.

For experiments shown in Fig. 2A (Peptide A), we estimated P_o and mean open time by half-amplitude thresholds but the $P_{substate}$ could not be estimated due to the abundance of unresolved flickering events.

Statistical Analysis

Data are shown as means ± S.E.M. of *n* measurements. Statistical comparisons between groups were performed with Student's t-test of paired differences. Differences were considered statistically significant at $P < 0.05$.

RESULTS

In this work, we studied the action of Peptide A added to the cytosolic surface of cardiac RyR2 reconstituted into planar lipid bilayers. Peptide A has been shown to have various effects on partially active skeletal channels [25] but its fast kinetics complicated the interpretation. Consequently, we determined the action of Peptide A on fully activated channels and compared it to that of ball peptides (which allow better time resolution due to their slower kinetics). A set of studies were also carried out on skeletal muscle RyR1 or with RyR2 in the absence of caffeine with comparable results (results not shown).

Differential effects of Peptide A, Shaker B and KIMFK on RyR2 channels

RyR2 channels were activated by Ca^{2+} and caffeine to lock the channels in high P_o mode [39]. Under these conditions, most channels were fully open ($P_o > 0.9$) and displayed a small number of gating events (few short closures), which allowed good characterization of peptide-induced blocking events.

Peptide A, Shaker B or KIFMK added to the cytosolic chamber decreased P_o of RyR2 in a voltage-dependent manner (Fig 1). We analyzed the voltage dependence of peptide block using a modified version of the equation derived by Woodhull [40] for block of a one-site, two-barrier channel model which has been shown to be applicable to RyR channels [41]:

$$P_{relative} = 1/[1 + ([Peptide]/K_{Pep}) \exp(dzV_m F/RT)]$$

where F, R, and T have their usual meanings, $P_{relative}$ is the ratio of open probabilities (presence of peptide/absence of peptide) measured at each voltage, and K_{Pep} is the peptide concentration at which block is half-maximal at 0 mV. dz is the "equivalent valence" of the blocker [40], influenced by z (blocker valence) and d (fraction of the membrane potential acting at the site), a term that includes binding site location within the membrane field, Ca^{2+} - peptide interactions in the pore and the possibility of multi-site peptide block.

From the data shown in Fig. 1, we estimated that Peptide A (z = 6) had a K_{Pep} = 4.30 ± 0.71 μM and d = 0.72 ± 0.11. Shaker B (z = 7) had similar K_{Pep} = 6.74 ± 0.94 μM and d = 0.82 ± 0.06. For KIFMK (z = 2) we estimated a larger K_{Pep} = 6.1 ± 0.3 mM and d = 1.2 ± 0.3. These results suggest that Shaker B and KIFMK block RyRs with similar affinity to their action on K^+ channels and Na^+ channels, respectively [33] and [42].

As shown in Fig. 2A, Peptide A-induced events at 0 mV were mostly fast flicker block (mean duration 0.81 ± 0.07 ms; *n*=4), which were not well resolved due to the filtering of data at 500–1000 Hz. For Shaker B, block events were longer (Fig. 2B), usually from ~100 milliseconds to seconds (mean block time at 0 mV = 1.18 ± 0.21 s; *n*=6). As Shown in Fig. 2C, KIFMK-induced block events had intermediate duration (compared to Peptide A and Shaker B). The mean block time at 0 mV was 5.3 ± 0.3 ms (*n*=6). Thus, Peptide A is a much faster blocker than Shaker B or KIFMK.

Channel transitions to subconductance states (substates) are a rare occurrence for RyR2 when Ca^{2+} is used as current carrier. Here, it was noticeable that all peptides induced substates, although with variable efficacy. Peptide A induced substates lasting a few milliseconds with low frequency but they were difficult to distinguish from the noise produced by the unresolved flicker block events (Fig. 2A). In the presence of the slower blocker Shaker B (2 μM), we detected low frequency of substates (Fig. 2B, upper right panel). At higher concentrations (20 μM), Shaker B blocked the channels ~85% of the time (0 mV) and half of the openings were to substates of ~50 and 70% of the full conductance (Fig. 3). Additionally, we detected transitions to substates of ~32% of the full conductance but their frequency was too low to produce a significant component in the amplitude distribution histograms. There is no strong correlation between induction of substates and the blocking kinetics of the peptides. Indeed, the peptides with fastest and slowest block kinetics (Peptide A and Shaker B) were both more effective in inducing substates than KIFMK. Frame by frame analysis of the recordings was required to evidence that KIFMK (500 μM) also increased frequency of substates 37 ± 9 times (from 0.9 ± 0.3 to 22.1 ± 4.4 events/min, n=5 paired observations). KIFMK-induced substate levels were ~27.3 ± 0.3, 48.6 ± 0.7 and 72.3 ± 0.5% of the full conductance. Notice, however, that the probability of substate events was extremely low and was not discernible from the noise in the current amplitude distribution histograms.

The results suggest that, although different peptide moieties can induce substates and block, the RyR2 conduction pore would kinetically discriminate between peptides (probably because of size, charges and hydrophobicity).

Ryanodine-modified RyR2 are more sensitive to the action of peptides

Ryanodine binds specifically to RyRs in a virtually irreversible manner, i.e. dissociation has an apparent $t_{1/2}$ of 8–25 hours [43] and [44]. Ryanodine locks the channels open in a modified state with slope conductance of ~40% that of full openings [3] and [45]. Studies with ryanoids indicated that, similar to peptides, they bind to a site that senses the electric field [46] and

[47]. If peptide-induced substates result from their reversible interaction with the "ryanoid site", then we should not observe these substates in ryanodine-modified channels (the "ryanoid site" would be occupied by ryanodine).

In the presence of ryanodine, channels are locked open; closures are brief and extremely rare (Fig. 2A, 2B, 2C and 2D, lower left panels). Paired studies of the action of Peptide A before and after addition of ryanodine are shown in Fig. 2A. Clearly, Peptide A became a more efficacious blocker after the channels were modified by ryanodine (Fig 2A, upper right versus lower right panels). In the presence of Peptide A, the fraction of time spent in the full open state by the control *versus* the ryanodine-modified channels decreased from 0.44 ± 0.02 to 0.10 ± 0.03 at 0 mV; from 0.65 ± 0.01 to 0.29 ± 0.05 at 10 mV and from 0.86 ± 0.08 to 0.53 ± 0.04 at 20 mV (*n*=4). This decrease in the probability of full openings (P_o) reflects an increase in both block and intermediate conductance states induced by Peptide A, as shown in the amplitude histograms (Fig. 2A, upper right versus lower right panels). In ryanodine-modified channels most events were brief and the signal-to-noise ratio was reduced due to the decreased conductance. Consequently, we were unable to quantitatively resolve between Peptide A-induced block events and substates.

The effects of Shaker B on fully activated RyR2 were similar to those found with Peptide A. As shown, in Fig 2B, upper panels, in the presence of Shaker B (2 μM), only one substate was significant at 0 mV (P_{sub}= 0.08 ± 0.004) but was less frequent at more positive voltages. In the ryanodine-modified channels, transitions to three distinct Shaker B-induced substates significantly increased (~40% of total openings; Fig 2B, lower panels). They had 30 ± 1%, 49 ± 2% and 74 ± 1% the amplitude of the full openings of the ryanodine-modified channel (n=4). These proportions are equivalent to those found for substates induced by 10-fold higher doses of Shaker B in non-modified channels (Fig. 3).

KIFMK also induced abundant substates in the ryanodine-modified RyR2 (Fig 2C, lower panels). Again, we observed three substates of 31 ± 1%, 51 ± 1% and 75 ± 1% of the amplitude of the full openings of the ryanodine-modified channel (n=8). Similar to Shaker B, these proportions are equivalent to those found for KIFMK in the absence of ryanodine (27 ± 1%, 52 ± 1% and 74 ± 2%, n=8). With ryanodine, the increase in the probability of KIFMK-induced substates is much more dramatic than the change in full block events (i.e., events that decrease channel current to baseline levels). Notice that although the frequency of block events did not increase, the block dwell time increased by 316 ± 62% (from 9.2 ± 2.2 ms to 29.9 ± 10.5 ms; n=6). Frame by frame analysis revealed the presence of KIFMK-induced substates of three distinct subconductance levels. However, one of them (of ~52% the ryanodine-modified conductance) was highly predominant and represented the most significant component in the histograms from 4 min recordings shown in Fig. 2C, lower right panel. The other two had lower frequency and in some cases, they could not be detected in the current amplitude distribution histograms.

In the presence of ryanodine, when we changed the holding potential from 0 mV to +20 mV, the probability of Shaker B-induced block decreased by 89% while the probability of Shaker B-induced substates decreased only by 48%. Similar results were observed with KIFMK. A change in voltage from 0 to +20 mV decreased P_{block} by 83% and $P_{substate}$ by 61%. The results indicate that peptide-induced block is more sensitive to voltage than the formation of peptide-induced substates, again suggesting that peptides produce block and substates by binding to different sites. Our results also suggest that block and substates are not specific to Peptide A and that the formation of peptide-induced substates does not represent peptide binding to the ryanoid site.

Ryanodine-modified RyR2 are more sensitive to the action of Imperatoxin A

The dual action of peptides (substates and block) complicates the interpretation of results. However, Imperatoxin A ($IpTx_A$) which has structural homology with Peptide A induces the formation of substates but does not block the channel [48]. Therefore, if the formation of $IpTx_A$-induced and peptide-induced substates result from the binding of these agents to a common site in the RyR, $IpTx_A$ could be a relevant tool to study the block and substate-inducing effects of peptides as two separate phenomena.

As shown in Fig. 2D (upper left panels), 20 nM $IpTx_A$ induced the formation of substates (~1/3 the full channel conductance) in a voltage dependent manner. Upon addition of ryanodine, $IpTx_A$ remained effective to induce "sub-substates". Figure 2D shows that the probability of $IpTx_A$-induced substate (P_{IpTxA}) was much higher in the ryanodine-modified RyRs than that observed in the non-modified channels (P_{IpTxA} increased from 0.51 ± 0.03 to 0.91 ± 0.02 at 0 mV; from 0.29 ± 0.02 to 0.92 ± 0.03 at +10 mV; from 0.09 ± 0.02 to 0.85 ± 0.03 at +20 mV and from 0.04 ± 0.01 to 0.59 ± 0.03 at 30 mV, n=5). Data collected at +10 mV also show that the increase in P_{IpTxA} correlates with a large increase in the substates' mean duration (from 1.8 ± 0.6 to 27.7 ± 10 s; n=5) and a modest but significant increase in the probability of the transition full open → P_{IpTxA} (from 10.3 ± 1.7 to 21.9 ± 3.6 events min^{-1}; *n=5*). Thus, ryanodine also increases the affinity for $IpTx_A$ in the RyR2. A similar increase in the affinity of all substate sites may also explain why peptide-induced substates have higher probability and are better discernable in the presence of ryanodine.

Imperatoxin A excludes peptides from the substate site

As both $IpTx_A$- and peptide-induced substates increase in the presence of ryanodine, we tested whether these agents interact with each other. Figures 4A and 4C (upper panels) show recordings of Ca^{2+}/caffeine-activated RyR2 exposed to 50 nM $IpTx_A$. Channels oscillate between full openings and the $IpTx_A$ substate. Closures are very rare during the full openings and are virtually zero during the $IpTx_A$ substate. Addition of 20 μM Peptide A (Fig. 4A, lower panels) induced marked flicker block during the full openings but not during $IpTx_A$ substates. A similar observation was made with 40 μM Shaker B (Fig. 4C, lower panels). During full openings, Shaker B produced long block events but no events were observed during $IpTx_A$-induced substates. However, as shown in Figs. 4B and 4D, the probability of finding the channel in the $IpTx_A$-induced substate decreased upon addition of Peptide A (from 0.78 ± 0.13 to 0.28 ± 0.11; *n*=4) or Shaker B (from 0.87 ± 0.01 to 0.30 ± 0.03; *n*=5). The results indicate that when $IpTx_A$ is bound to the RyR2, it prevents the block and substate-inducing actions of peptides. This suggests that $IpTx_A$ and Shaker B/Peptide A compete for a common binding site.

As found for Shaker B and Peptide A, KIFMK did not induce sub-substates during the $IpTx_A$-induced events. This again suggests that $IpTx_A$ binding prevents access to the substate-inducing site. Unlike Peptide A and Shaker B, KIFMK was able to block the $IpTx_A$-modified channel (Fig. 5) suggesting that the $IpTx_A$ binding site and the blocking site might be different. Notice that in the recordings shown in Fig. 5A, block events during $IpTx_A$-induced substates are much longer than during channel full openings (Fig. 5B). The apparent dissociation constant of KIFMK from RyR2 (1/dwell time) decreased from 166 sec^{-1} during full openings to 3.1 sec^{-1} during $IpTx_A$ substates. However, KIFMK-induced block events were much less abundant during $IpTx_A$ substates (Fig. 5C), indicating a much larger decrease in the rate of association. As a consequence, the probability of blocking the channels was significantly lower during $IpTx_A$-induced substates than during full openings (Fig. 5D).

$IpTx_A$ also counteracted the action of peptides on the ryanodine-modified RyR2. During $IpTx_A$-ryanodine "sub-substates", Peptide A and Shaker B were ineffective and KIFMK only induced some block events (results not shown).

In summary, the results shown in this section indicate that $IpTx_A$ binding impedes the access of the large peptides (Peptide A/Shaker B) to the “substates" and "block" sites. The smaller peptide KIFMK can still access the block site suggesting that $IpTx_A$ does not compete for its occupancy. However, $IpTx_A$ increased the energy barrier for KIFMK binding and then stabilizing the peptide at the block site. These results also suggest that the Peptide A “block site” may be located deeper than the “substates site” in the RyR2 region that senses the electric field.

Cooperative interaction of ryanoids with peptides and Imperatoxin A

The possibility that Peptide A and $IpTx_A$ affect the affinity of RyR2 for ryanoids was also tested using ryanodol. As ryanodol reversibly binds to the ryanodine-binding site [46], RyR2 reversibly fluctuated between the full opening and the ryanodol-modified state (Fig. 6A, left panels). Ryanodol action is voltage-dependent [47]. When we changed voltage from 0 to +20mV the probability of ryanodol modification decreased by 52 ± 11% (n=6). Figure 6A (right panels) shows that Peptide A was more efficient to block the channel and induce substates during ryanodol-modified events versus full openings. This is similar to the results obtained with and without ryanodine (Fig. 2A). The additional information provided by Fig. 6B is that the probability of ryanodol-induced modification increased upon addition of Peptide A (from 0.58 ± 0.04 to 0.76 ± 0.05). This correlates with increased dwell times for ryanodol-modified states (Fig. 6B). This suggests that Peptide A stabilizes ryanodol bound to RyR2 by decreasing its rate of dissociation.

A similar increase in the probability of ryanodol modification was evident with $IpTx_A$. As shown in Fig. 7A (left panels) and Fig. 7B (upper panels), under control conditions the channel is switching between the full opening (Probability ~80%) and the ryanodol state (Probability ~ 20%). After the addition of $IpTx_A$, we observed full openings and three states (from higher to lower conductance): ryanodol (R), $IpTx_A$ (i) and $IpTx_A$ plus ryanodol (i+R). The total probability of ryanodol binding to RyR2 (R and R+i) increased (~40%). This was true at all voltages tested but +30 mV, where $IpTx_A$ and ryanodol bindings have low probability (Fig. 7B and 7C). Notice, however, that in all cases the probability of R (ryanodol alone) decreased dramatically. Thus, when ryanodol binds, $IpTx_A$ follows, stabilizing the channel in R+i (Fig. 7C). These results, as well as those in Fig. 2 (increase in the actions of peptides or $IpTx_A$ with ryanodine), suggest that peptides/$IpTx_A$ cooperatively interact with ryanoids stabilizing each other’s association to RyR2.

Additional analysis of data suggests that initial binding of ryanodol or $IpTx_A$ had opposite effects on the probability of reaching R+i. Figure 7D shows estimations (from 40 minutes of recordings at +10 mV) of the probability of full openings, R, i, and R+i substates. The data indicates that the channels spend more time in the $IpTx_A$ alone state (~41% of the time) than in i+R state (30%). This seems to be in contrast with the idea of a more stable R+i state. However, it can be explained by the existence of a preferential order in the sequence by which both agents (ryanodol and $IpTx_A$) bind to RyR2. The arrows show RyR2 transitions from one state to another. From the number of events, we can determine that channels residing in R substates (98 events) are much more likely to change to the R+i substate (93 times) than back to the full open state (5 times). In contrast, channels in the $IpTx_A$ substate (873 events) frequently changed back to the open state (867 times) but only rarely to the R+i substate (6 times). Relative rate of transition (number of transitions A→B/probability A) for R→R+i (4650) nearly doubled that for Open→i (2780). More important, the rate of the transition R +i→R (218) was much lower than that of i→Open (2114). This again indicates stabilization of $IpTx_A$ binding during the R substates. Contrarily, the rate for Open→R (130) is much higher than that of i→R+i (14.6), suggesting that when $IpTx_A$ binds first, it prevents ryanodol binding. Thus, there is a preferred sequence of binding Open→R→R+i (93% of the cases). This

asymmetry is much less evident for the transitions R+i→i (144) vs. R+i→R (218), which suggests that R and i dissociation from RyR2 does not have a preferred sequence.

DISCUSSION

We found that Peptide A could interact with sites in the RyR2 conduction pathway to induce substates and block. This action was enhanced by ryanoids. Concomitantly, the affinity of the ryanoid site for its ligands increased, suggesting that Peptide A and ryanoids cooperatively interact.

The action of Peptide A was prevented by Imperatoxin-A ($IpTx_A$) a compound that induced one single type of substate and did not induce RyR2 channel block. $IpTx_A$ also stabilized ryanodol bound to the RyR2. However, when $IpTx_A$ binds first, it prevents the access of ryanodol to its binding site.

The voltage-gated channel ball peptides (Shaker B and KIFMK) also induced voltage-dependent block and substates that were sensitive to ryanoids and $IpTx_A$.

Peptide A occludes the RyR2 pore

Previous studies have shown various effects of Peptide A on skeletal RyR1 [16], [17], [18], [23], [25], [26], [27] and [28]. However, skeletal RyR1 channels have variable levels of activity, voltage dependence and modal gating and are usually reconstituted as multichannels [38]. In our hands, this inherent complexity of RyR1 behavior precluded good quantization of the action of Peptide A [34].

Cardiac RyR2 channels can be frequently reconstituted as single channels and are much more homogeneous [38]. Therefore, we tested the action of Peptide A, Shaker B and KIFMK on fully active RyR2, locked in "high P_o" mode by caffeine [39]. Under these conditions, Peptide A induced both flicker block and short lived intermediate states of conductance (substates). Shaker B and KIFMK had similar action (block and substates) but slower kinetics ("slow block") on RyR2. This made it possible to resolve well defined substate levels of ~30, 50 and 70% of the full RyR2 conductance. Peptides and $IpTx_A$ had a qualitatively similar action on RyR2 in the absence of caffeine (results not shown). Under these conditions, however, quantization of block events cannot be attained due to the interference by normal events of RyR2 alternating between gating modes characterized by long openings with abundant rapid closures, inactivity or flickering openings.

Ryanodine-modification may increase the affinity of a vestibular "substate site" to peptides

Our studies indicated that peptides and $IpTx_A$ interact with "substate site(s)" located in a region that is less sensitive to the transmembrane electric field than the "block site". These peptide-induced substates do not represent binding to a ryanoid site ryanodine modification dramatically stabilized peptide- and $IpTx_A$ induced substates. Furthermore, the ratio (amplitude of sublevel/amplitude full openings) of peptide- or $IpTx_A$-induced substates at $V_m \geq 0$ mV was the same in the presence versus absence of ryanodine modification. This suggests that the effects of ryanodine and $IpTx_A$ / peptides on channel conductance result from two separate and additive processes.

Ryanodine induces a large conformational change in the RyR channel molecule [49]. and “lock open” the RyR in a modified state of conductance [3] and [45]. Our results suggest that such conformational and/or gating changes increase the affinity of the “substate” site(s) for peptides.

Substates are a common observation in single-channel studies but it is still unknown if they represent partial occlusion of a pore, conformational changes or uncoupling of multipores [50], [51] and [52].

It is thought that tetrameric K^+ channels with identical subunits have four pores that transition in synchrony from closed to open by the fast coupled movement of four voltage sensors [51]. It has been suggested that substates represent the rare occasions where voltage sensors uncouple [51].

The presence of voltage sensors in RyR has been previously suggested [53]. If the structural homology detected between RyRs and voltage-gated channels [31] extends to these gates, our results would suggest that Peptide A interacts with them. The role of these sensors on RyR2 function remains unclear, since changes in SR membrane potential during EC-coupling are unlikely (reviewed in [2]). However, it is possible that voltage changes at the t-tubule membrane are sensed by Peptide A (or other moieties) of the DHPR which, in turn, interact with gates of RyR2.

Imperatoxin A prevents occupancy of Peptide A and ryanoid sites

Our results would suggest that $IpTx_A$ can bind to a vestibular "substate" site but it cannot reach the “block” site. This could be related to its larger size (compared to the other peptides tested here) or to its more rigid structure [54].

Previous reports suggested that $IpTx_A$ and Peptide A interfere with each-other’s actions on RyR2 [17], [18], [22], [23] and [54]. Accordingly, we found that $IpTx_A$ binding prevents Peptide A (and ball peptides) -induced substates and peptide-induced block in both control and ryanodine-modified channels. During $IpTx_A$-induced substates, the smaller KIFMK was still able to block the channel, suggesting that $IpTx_A$ does not compete for occupancy of the site. These block events were much less frequent (suggesting increased activation energy to access the block site) and had longer dwell times (indicating increased affinity for occupancy of the site).

In summary, $IpTx_A$ bound to RyR2 would behave as a gate that (either sterically or allosterically) prevents the entrance of Peptide A / ball peptides to their substate and block sites.

Peptide A increases affinity of the RyR2 ryanoid site for its ligands

Another novel observation in this article is that ryanoids and peptides cooperatively interact. Ryanodol and $IpTx_A$ also stabilized each other’s binding to RyR2, i.e., the apparent affinities for their binding sites are increased. Since $IpTx_A$ did not induce block, we were able to determine that there is a preferential sequence of binding. This suggests that the ryanoid site, similar to the block site, is sensitive to the action of $IpTx_A$ as a gate.

These results also warn us against a possible pitfall of using "non-equilibrium" [^{3}H] ryanodine binding [44] to estimate changes in P_o of RyRs exposed to open-pore blockers or agents that induce substates. Here, open RyR2 (P_o ~0.99) were blocked by Peptide A or modified by $IpTx_A$ and displayed an increased affinity for ryanoids. These interactions between Peptide A and ryanoid sites may explain why Peptide A enhances [^{3}H] ryanodine binding to SR microsomes ([19], [26] and [55]) while, at similar levels, it inhibits SR Ca^{2+} release [26].

Is there a physiological role for "Peptide A -like" modulation of RyR channels?

Previous studies in skeletal muscle and heart support the idea that a mechanism of negative control of RyRs exists in striated muscle that involves DHPR [9], [10], [11], [12], [13] and

[14], which can even hold ryanodine-modified RyRs from releasing Ca^{2+} in skeletal fibers at rest [56]. The present work and previous studies show that Peptide A from the DHPR II–III loop could effectively act as a "ball peptide" for RyR2 [27] and [28]. Although a significant role of Peptide A during EC-coupling is not apparent in skeletal fibers [57], it is still possible that other "ball-peptide like" moieties in DHPR or associate molecules participate of the negative modulation of RyRs.

Native RyRs studied in heart and muscle cells have a much lower (up to ~10,000 times) affinity for $IpTx_A$ than that of isolated channels reconstituted in bilayers [58] and [59]. Moreover, DHPR peptides do not affect the magnitude and duration of Ca^{2+} sparks [13]. These results suggest that in cells, some moiety restricts the access of $IpTx_A$ and peptides to their binding sites in the RyR2.

In summary, our results and previous reports suggest the possibility of a role for “ball peptides” in the negative control of RyR-mediated Ca^{2+} leak under resting conditions or to terminate RyR-induced Ca^{2+} release during EC-coupling. However, the putative moiety responsible for this action in cells still needs to be identified.

ACKNOWLEDGMENTS

This work was supported by the National Institutes of Health (R01 GM078665, to JAC and R01HL071741 to JRF) and the Muscular Dystrophy Association (MDA3699 to JAC). The authors would like to thank Dr. Amy Arai for her critical input and Mrs. Judy Bryan for proofreading the manuscript.

REFERENCES

1. Lamb GD. Excitation-contraction coupling in skeletal muscle: comparisons with cardiac muscle. Clin. Exp. Pharmacol. Physiol 2000;27:216–224. [PubMed: 10744351]
2. Bers, DM. Excitation-Contraction Coupling and Cardiac Contractile Force. Vol. 2nd Ed. Dordrecht, The Netherlands: Kluwer Academic Press; 2001.
3. Fill M, Copello JA. Ryanodine receptor calcium release channels. Physiol. Rev 2002;82:893–922. [PubMed: 12270947]
4. Chamberlain BK, Levitsky DO, Fleischer S. Isolation and characterization of canine cardiac sarcoplasmic reticulum with improved Ca^{2+} transport properties. J. Biol. Chem 1983;258:6602–6609. [PubMed: 6304048]
5. Lai FA, Erickson HP, Rousseau E, Liu QY, Meissner G. Purification and reconstitution of the calcium release channel from skeletal muscle. Nature 1988;331:315–319. [PubMed: 2448641]
6. Sitsapesan, R.; Williams, A. The structure and function of ryanodine receptors. London: Imperial College Press; 1998.
7. Meissner G. Molecular regulation of cardiac ryanodine receptor ion channel. Cell Calcium 2004;35:621–628. [PubMed: 15110152]
8. Stern MD, Cheng H. Putting out the fire: what terminates calcium-induced calcium release in cardiac muscle? Cell Calcium 2004;35:591–601. [PubMed: 15110149]
9. Franzini-Armstrong C. Functional implications of RyR-dHPR relationships in skeletal and cardiac muscles. Biol. Res 2004;37:507–512. [PubMed: 15709676]
10. Bers DM, Stiffel VM. The ratio of ryanodine: dihydropyridine receptors in cardiac and skeletal muscle and implications for E-C coupling. Am. J. Physiol 1993;264:C1587–C1593. [PubMed: 8333507]
11. Zhou J, Yi J, Royer L, Launikonis BS, Gonzalez A, Garcia J, Rios E. A probable role of dihydropyridine receptors in repression of Ca^{2+} sparks demonstrated in cultured mammalian muscle. Am. J. Physiol. Cell. Physiol 2006;290:C539–C553. [PubMed: 16148029]
12. Katoh H, Schlotthauer K, Bers DM. Transmission of information from cardiac dihydropyridine receptor to ryanodine receptor: evidence from BayK 8644 effects on resting Ca^{2+} sparks. Circ. Res 2000;87:106–111. [PubMed: 10903993]

13. Li Y, Bers DM. A cardiac dihydropyridine receptor II–III loop peptide inhibits resting Ca^{2+} sparks in ferret ventricular myocytes. J. Physiol 2001;537:17–26. [PubMed: 11711557]
14. Copello JA, Zima AV, Diaz-Sylvester PL, Fill M, Blatter LA. Ca^{2+} entry-independent effects of L-type Ca^{2+} channel modulators on Ca^{2+} sparks in ventricular myocytes. Am. J. Physiol. Cell. Physiol 2007;292:C2129–C2140. [PubMed: 17314267]
15. Lu X, Xu L, Meissner G. Activation of the skeletal muscle calcium release channel by a cytoplasmic loop of the dihydropyridine receptor. J. Biol. Chem 1994;269:6511–6516. [PubMed: 8120002]
16. el-Hayek R, Antoniu B, Wang J, Hamilton SL, Ikemoto N. Identification of calcium release-triggering and blocking regions of the II–III loop of the skeletal muscle dihydropyridine receptor. J. Biol. Chem 1995;270:22116–22118. [PubMed: 7673188]
17. Gurrola GB, Arevalo C, Sreekumar R, Lokuta AJ, Walker JW, Valdivia HH. Activation of ryanodine receptors by imperatoxin A and a peptide segment of the II–III loop of the dihydropyridine receptor. J. Biol. Chem 1999;274:7879–7886. [PubMed: 10075681]
18. Casarotto MG, Green D, Pace SM, Curtis SM, Dulhunty AF. Structural determinants for activation or inhibition of ryanodine receptors by basic residues in the dihydropyridine receptor II–III loop. Biophys. J 2001;80:2715–2726. [PubMed: 11371447]
19. Yamamoto T, Rodriguez J, Ikemoto N. Ca^{2+}-dependent dual functions of peptide C. The peptide corresponding to the Glu724-Pro760 region (the so-called determinant of excitation-contraction coupling) of the dihydropyridine receptor alpha 1 subunit II–III loop. J. Biol. Chem 2002;277:993–1001. [PubMed: 11682472]
20. Haarmann CS, Green D, Casarotto MG, Laver DR, Dulhunty AF. The random-coil 'C' fragment of the dihydropyridine receptor II–III loop can activate or inhibit native skeletal ryanodine receptors. Biochem. J 2003;372:305–316. [PubMed: 12620094]
21. Bannister ML, Williams AJ, Sitsapesan R. Removal of clustered positive charge from dihydropyridine receptor II–III loop peptide augments activation of ryanodine receptors. Biochem. Biophys. Res. Commun 2004;314:667–674. [PubMed: 14741687]
22. Dulhunty AF, Karunasekara Y, Curtis SM, Harvey PJ, Board PG, Casarotto MG. The recombinant dihydropyridine receptor II–III loop and partly structured 'C' region peptides modify cardiac ryanodine receptor activity. Biochem. J 2005;385:803–813. [PubMed: 15511220]
23. Altafaj X, Cheng W, Esteve E, Urbani J, Grunwald D, Sabatier JM, Coronado R, De Waard M, Ronjat M. Maurocalcine and domain A of the II–III loop of the dihydropyridine receptor Cav 1.1 subunit share common binding sites on the skeletal ryanodine receptor. J. Biol. Chem 2005;280:4013–4016. [PubMed: 15591063]
24. Bannister ML, Ikemoto N. Effects of peptide C corresponding to the Glu724-Pro760 region of the II–III loop of the DHP (dihydropyridine) receptor alpha1 subunit on the domain- switch-mediated activation of RyR1 (ryanodine receptor 1) Ca^{2+} channels. Biochem. J 2006;394:145–152. [PubMed: 16302848]
25. Dulhunty AF, Laver DR, Gallant EM, Casarotto MG, Pace SM, Curtis S. Activation and inhibition of skeletal RyR channels by a part of the skeletal DHPR II–III loop: effects of DHPR Ser687 and FKBP12. Biophys. J 1999;77:189–203. [PubMed: 10388749]
26. Chen L, Esteve E, Sabatier JM, Ronjat M, De Waard M, Allen PD, Pessah IN. Maurocalcine and peptide A stabilize distinct subconductance states of ryanodine receptor type 1, revealing a proportional gating mechanism. J. Biol. Chem 2003;278:16095–16106. [PubMed: 12586831]
27. Dulhunty AF, Curtis SM, Cengia L, Sakowska N, Casarotto MG. Peptide fragments of the dihydropyridine receptor can modulate cardiac ryanodine receptor channel activity and sarcoplasmic reticulum Ca^{2+} release. Biochem. J 2004;379:161–172. [PubMed: 14678014]
28. Dulhunty AF, Curtis SM, Watson S, Cengia L, Casarotto MG. Multiple actions of imperatoxin A on ryanodine receptors: interactions with the II–III loop "A" fragment. J. Biol. Chem 2004;279:11853–11862. [PubMed: 14699105]
29. Gyorke S, Velez P, Suarez-Isla B, Fill M. Activation of single cardiac and skeletal ryanodine receptor channels by flash photolysis of caged Ca^{2+} Biophys. J 1994;66:1879–1886. [PubMed: 8075325]
30. Velez P, Gyorke S, Escobar AL, Vergara J, Fill M. Adaptation of single cardiac ryanodine receptor channels. Biophys. J 1997;72:691–697. [PubMed: 9017196]

31. Williams AJ, West DJ, Sitsapesan R. Light at the end of the Ca($^{2+}$)-release channel tunnel: structures and mechanisms involved in ion translocation in ryanodine receptor channels. Q. Rev. Biophys 2001;34:61–104. [PubMed: 11388090]
32. Mead FC, Sullivan D, Williams AJ. Evidence for negative charge in the conduction pathway of the cardiac ryanodine receptor channel provided by the interaction of K+ channel N-type inactivation peptides. J. Membr. Biol 1998;163:225–234. [PubMed: 9625779]
33. Wang SY, Wang GK. Block of inactivation-deficient cardiac Na^+ channels by acetyl-KIFMK-amide. Biochem. Biophys. Res. Commun 2005;329:780–788. [PubMed: 15737654]
34. Porta M, Nani A, Ramos-Franco J, Fill M, Ikemoto N, Copello J. Modulation of ryanodine receptors (RyRs) channels by dihydropyridine receptor (DHPR) peptide A (PepA). Biophys. J 2003;84a2078-Pos
35. Diaz-Sylvester PL, Porta M, Escobar AL, Copello JA. Voltage dependent modulation of ryanodine receptors (RyRs) by peptide probes. Biophys. J 2007;88a:408-Pos.
36. Deslongchamps P, Bélanger A, Berney DJF, Borschberg HJ, Brousseau R, Doutheau A, Durand R, Katayama H, Lapalme R, Leturc DM, Soucy P, Liao CC, MacLachlan FN, Maffrand JP, Marazza F, Martino R, Moreau C, Ruest L, Saint-Laurent L, Saintonge R, Soucy P. The total synthesis of (1)-ryanodol. Can. J. Chem 1990;68:115–192.
37. Saito A, Seiler S, Chu A, Fleischer S. Preparation and morphology of sarcoplasmic reticulum terminal cisternae from rabbit skeletal muscle. J. Cell. Biol 1984;99:875–885. [PubMed: 6147356]
38. Copello JA, Barg S, Onoue H, Fleischer S. Heterogeneity of Ca^{2+} gating of skeletal muscle and cardiac ryanodine receptors. Biophys. J 1997;73:141–156. [PubMed: 9199779]
39. Sitsapesan R, Williams AJ. Mechanisms of caffeine activation of single calcium-release channels of sheep cardiac sarcoplasmic reticulum. J. Physiol 1990;423:425–439. [PubMed: 2167363]
40. Woodhull AM. Ionic blockage of sodium channels in nerve. J. Gen. Physiol 1973;61:687–708. [PubMed: 4541078]
41. Mead F, Williams AJ. Block of the ryanodine receptor channel by neomycin is relieved at high holding potentials. Biophys. J 2002;82:1953–1963. [PubMed: 11916853]
42. Li W, Aldrich RW. State-dependent block of BK channels by synthesized shaker ball peptides. J. Gen. Physiol 2006;128:423–441. [PubMed: 16966472]
43. Pessah IN, Stambuk RA, Casida JE. Ca^{2+}-activated ryanodine binding: mechanisms of sensitivity and intensity modulation by Mg^{2+}, caffeine, and adenine nucleotides. Mol. Pharmacol 1987;31:232–238. [PubMed: 2436032]
44. Chu A, Díaz-Muñoz M, Hawkes MJ, Brush K, Hamilton SL. Ryanodine as a probe for the functional state of the skeletal muscle sarcoplasmic reticulum calcium release channel. Mol. Pharmacol 1990;37:735–741. [PubMed: 1692609]
45. Rousseau E, Smith JS, Meissner G. Ryanodine modifies conductance and gating behavior of single Ca^{2+} release channel. Am. J. Physiol 1987;253:C364–C368. [PubMed: 2443015]
46. Tinker A, Sutko JL, Ruest L, Deslongchamps P, Welch W, Airey JA, Gerzon K, Bidasee KR, Besch HR Jr, Williams AJ. Electrophysiological effects of ryanodine derivatives on the sheep cardiac sarcoplasmic reticulum calcium-release channel. Biophys. J 1996;70:2110–2119. [PubMed: 9172735]
47. Tanna B, Welch W, Ruest L, Sutko JL, Williams AJ. The interaction of a neutral ryanoid with the ryanodine receptor channel provides insights into the mechanisms by which ryanoid binding is modulated by voltage. J. Gen. Physiol 2000;116:1–9. [PubMed: 10871634]
48. Tripathy A, Resch W, Xu L, Valdivia HH, Meissner G. Imperatoxin A induces subconductance states in Ca^{2+} release channels (ryanodine receptors) of cardiac and skeletal muscle. J. Gen. Physiol 1998;111:679–690. [PubMed: 9565405]
49. Orlova EV, Serysheva II, van Heel M, Hamilton SL, Chiu W. Two structural configurations of the skeletal muscle calcium release channel. Nat. Struct. Biol 1996;3:547–552. [PubMed: 8646541]
50. Dani JA, Fox JA. Examination of subconductance levels arising from a single ion channel. J. Theor. Biol 1991;153:401–423. [PubMed: 1724679]
51. Chapman ML, VanDongen AM. K channel subconductance levels result from heteromeric pore conformations. J. Gen. Physiol 2005;126:87–103. [PubMed: 16043772]

52. Basle A, Iyer R, Delcour AH. Subconductance states in OmpF gating. Biochim. Biophys. Acta 2004;1664:100–107. [PubMed: 15238263]

53. Ma J. Desensitization of the skeletal muscle ryanodine receptor: evidence for heterogeneity of calcium release channels. Biophys. J 1995;68:893–899. [PubMed: 7756554]

54. Lee CW, Lee EH, Takeuchi K, Takahashi H, Shimada I, Sato K, Shin SY, Kim DH, Kim JI. Molecular basis of the high-affinity activation of type 1 ryanodine receptors by imperatoxin A. Biochem. J 2004;377:385–394. [PubMed: 14535845]

55. Simeoni I, Rossi D, Zhu X, Garcia J, Valdivia HH, Sorrentino V. Imperatoxin A (IpTx(a)) from Pandinus imperator stimulates [^{3}H]ryanodine binding to RyR3 channels. FEBS Lett 2001;508:5–10. [PubMed: 11707258]

56. Hui CS, Bidasee KR, Besch HR Jr. Effects of ryanodine on calcium sparks in cut twitch fibres of Rana temporaria. J. Physiol 2001;534:327–342. [PubMed: 11454954]

57. Ahern CA, Bhattacharya D, Mortenson L, Coronado R. A Component of excitation-contraction coupling triggered in the absence of the T671-L690 and L720-Q765 regions of the II–III loop of the Dihydropyridine receptor alpha 1s pore subunit. Biophys. J 2001;81:3294–3307. [PubMed: 11720993]

58. Terentyev D, Viatchenko-Karpinski S, Valdivia HH, Escobar AL, Gyorke S. Luminal Ca^{2+} controls termination and refractory behavior of Ca^{2+}-induced Ca^{2+} release in cardiac myocytes. Circ. Res 2002;91:414–420. [PubMed: 12215490]

59. Schneider MF, Rodney GG. Peptide and protein modulation of local Ca^{2+} release events in permeabilized skeletal muscle fibers. Biol. Res 2004;37:613–616. [PubMed: 15709689]

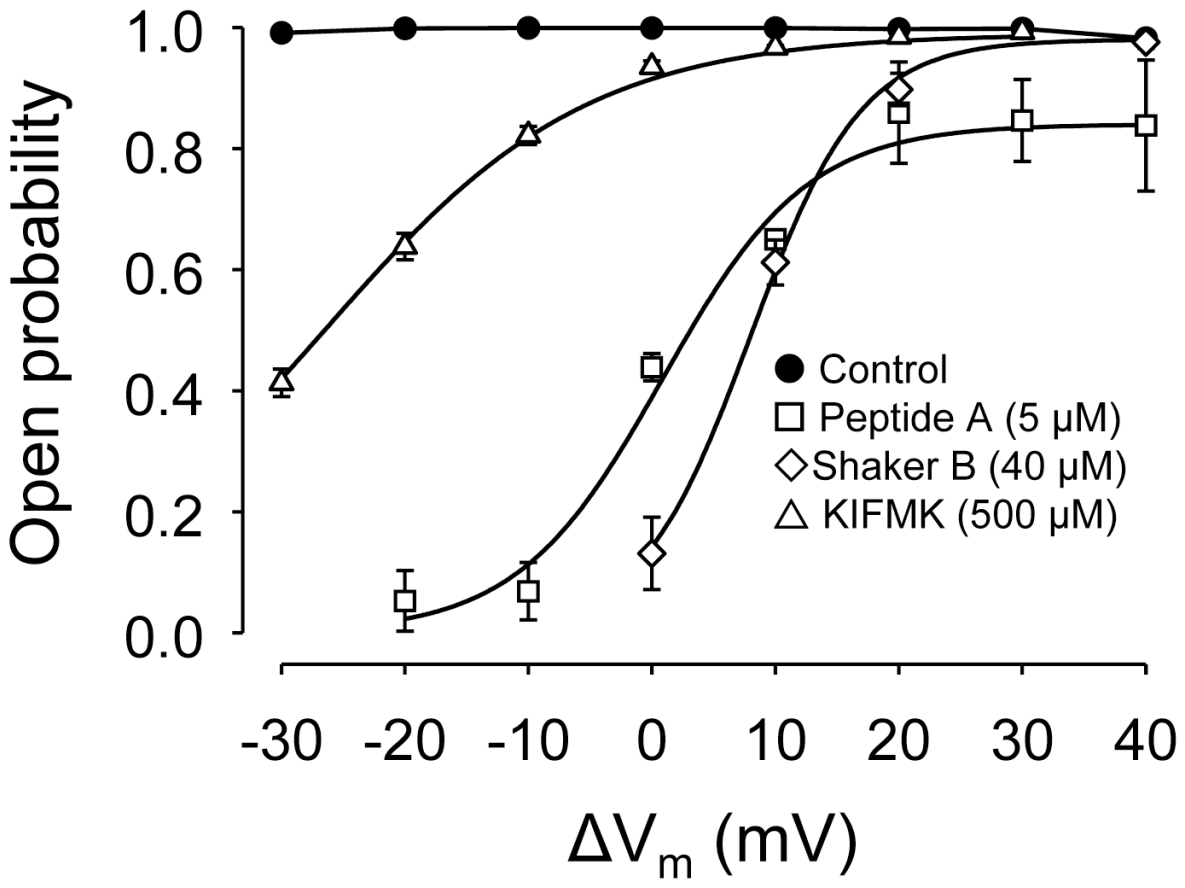

Fig. 1.

Peptides block RyR2 in a voltage-dependent manner. Mean open probability (P_o) of RyR2 channels as a function of holding voltage (V_m) ranging from −30 mV to +40 mV (trans - cis). RyR2 channels were fully activated by the combined action of Ca^{2+} (10 μM) and caffeine (5 mM) in their cytosolic (cis) surface. Lumenal (trans) Ca^{2+} (50 mM) was the current carrier. Po's are mean values from n = 15 (control; filled circles), 4 (Peptide A, open squares), 6 (Shaker B, open diamonds) and 6 (KIFMK; open triangles). Values are shown as mean ± SEM. Lines represent fits of the Woodhull equation to experimental data (see Results).

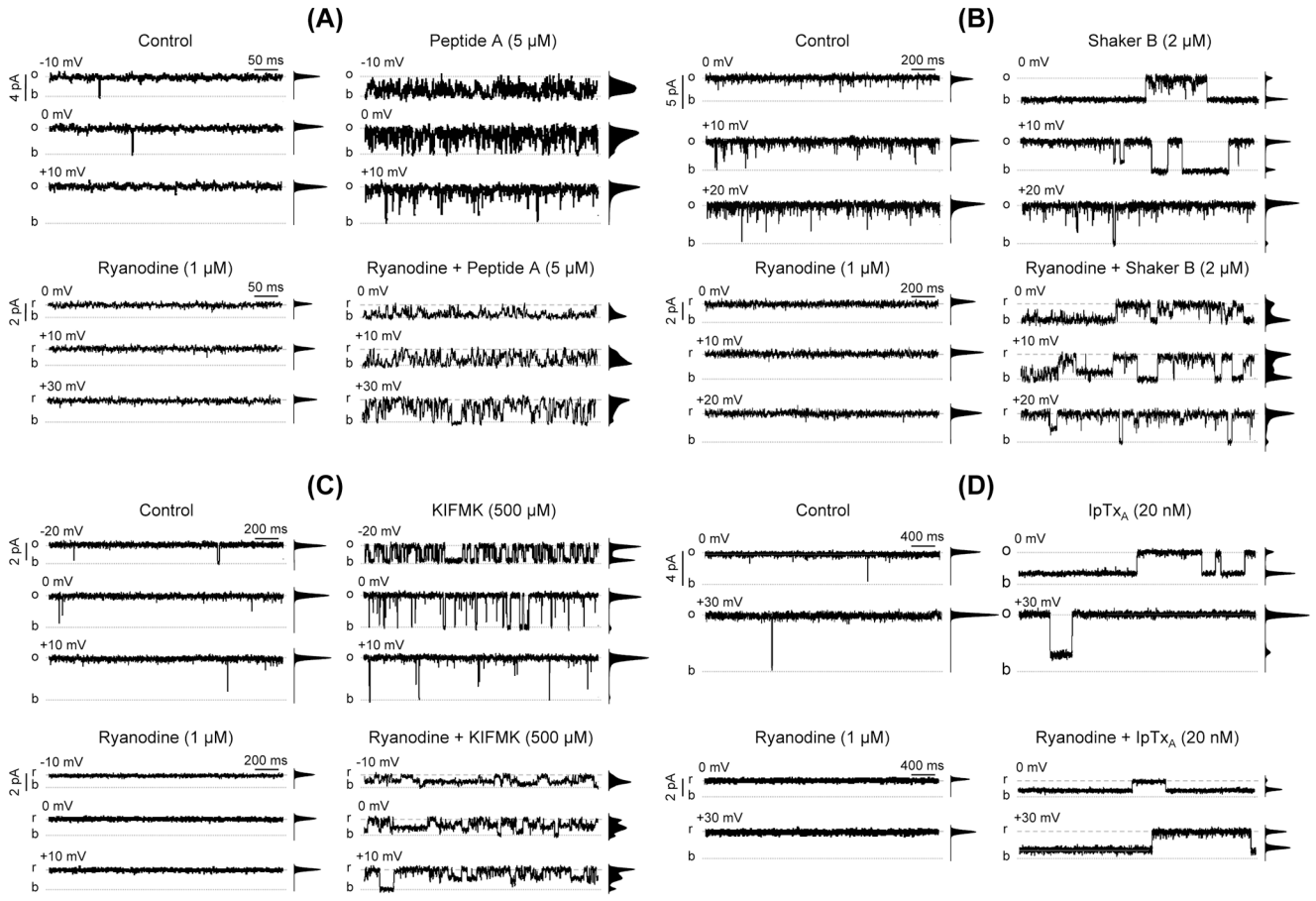

Fig. 2.

Ryanodine modifies the action of peptides and of Imperatoxin A. The figure shows single-channel recordings of single RyR2 channels activated with Ca^{2+}/caffeine. Openings are shown as upward deflections (o = full open; b = baseline). The frequency-current amplitude histograms obtained from 4 min single-channel recordings are shown next to each trace. The figure shows the effects of (A) 5 μM Peptide A, (B) 2 μM Shaker B, (C) 500 μM KIFMK and (D) 20 nM Imperatoxin A. In all cases four panels are shown. *Upper panels*. Representative traces recorded at the indicated voltages in the absence of ryanodine under control conditions (upper left panels) and after addition of 5 μM Peptide A, 2 μM Shaker B, 500 μM KIFMK or 20 nM Imperatoxin A (upper right panels in A, B, C and D, respectively). *Lower panels*. Single RyR2 channel recordings after modification by ryanodine (2 μM). r represents full openings to the ryanodine-modified state. Traces are shown under control conditions (lower left panels) and after addition of Peptide A, Shaker B, KIFMK or Imperatoxin A (lower right panels in A, B, C and D, respectively).

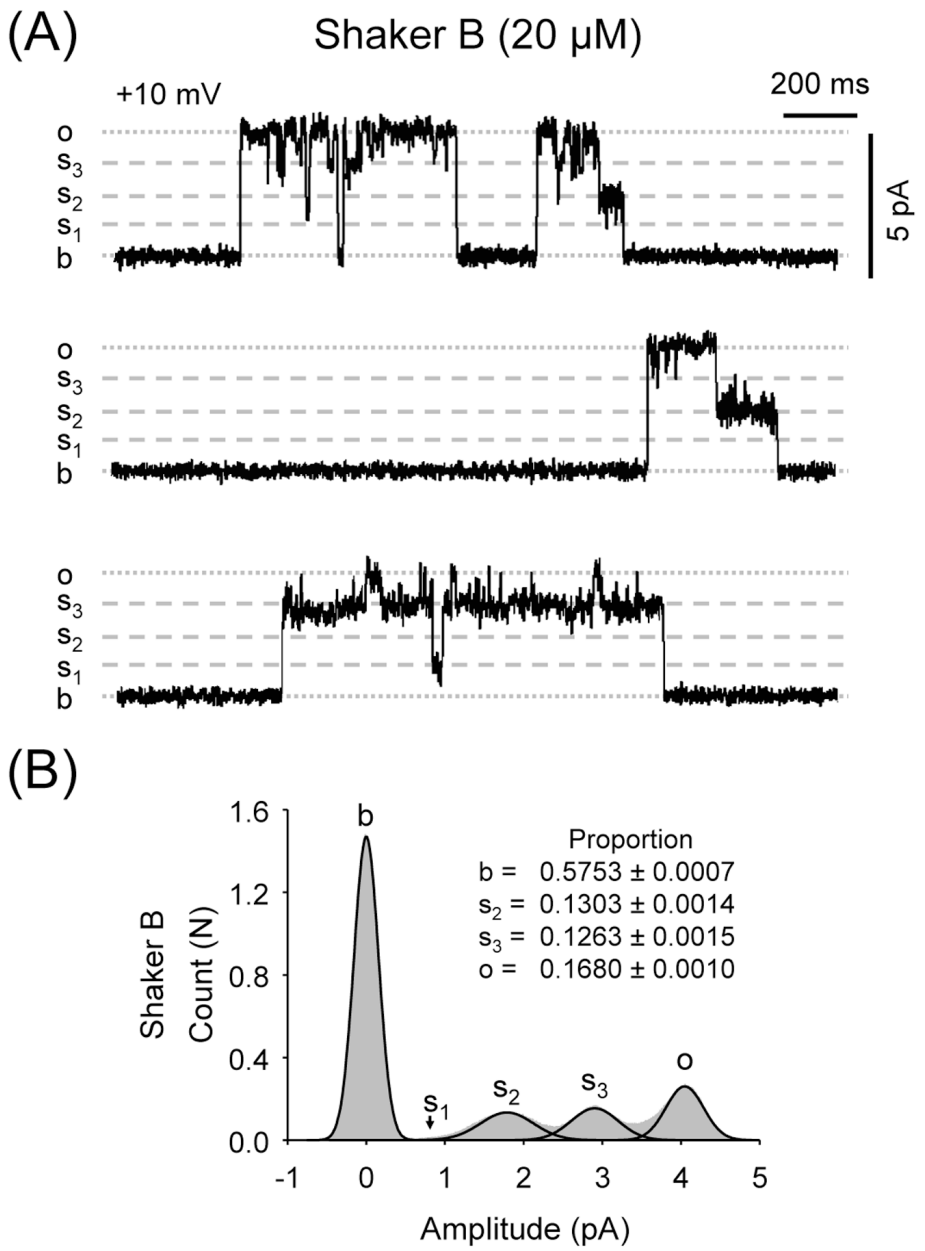

Fig. 3.

High doses of Shaker B induce three distinct levels of subconductance. (A) RyR2 recordings of a Ca^{2+}/caffeine-activated channel at Vm = +10 mV in the presence of 20 µM Shaker B. s_1, s_2 and s_3 indicate the conductance of the different substates. (B) Amplitude histograms and fits of RyR2 channels exposed to 20 µM Shaker B.

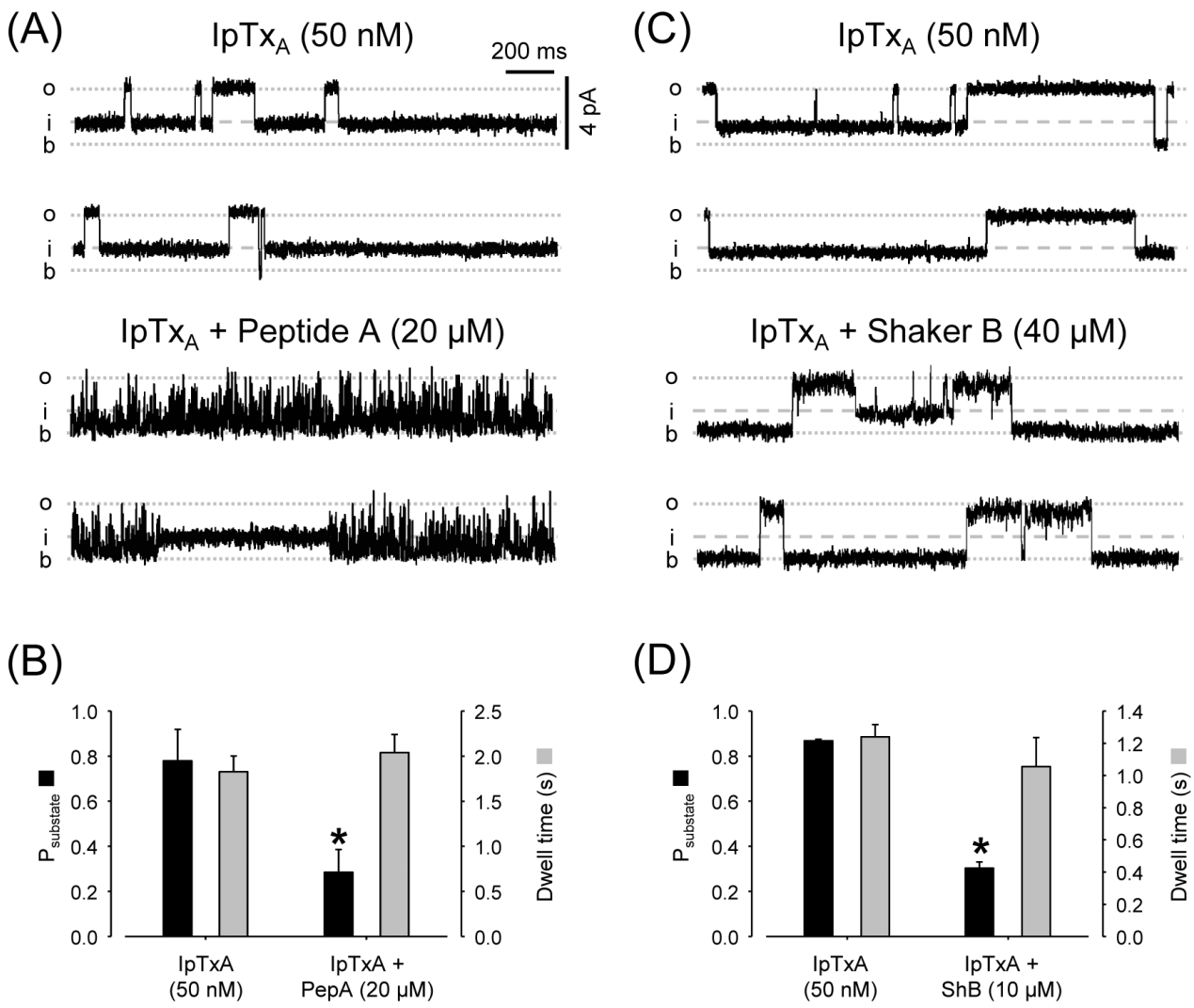

Fig. 4.

Mutual exclusion of Imperatoxin versus Peptide A or Shaker B. (A) Single-channel recordings of RyR2 with Ca^{2+}/caffeine and IpTx$_A$ (50 nM) at Vm = +10 mV. Traces under control conditions (top) and after adding 20 μM Peptide A (bottom). (B) Probability (P$_{substate}$; black bars) and dwell time (grey bars) of imperatoxin-induced substates before and after addition of Peptide A. * $p < 0.05$, n=5 paired observations. (C) RyR2 recordings in presence of Ca^{2+}/ caffeine and IpTx$_A$ (50 nM); Vm = +10 mV. Traces are shown in the absence (control; conditions (top) and presence of 40 μM Shaker B (bottom). (D) Probability (P$_{substate}$; black bars) and dwell time (grey bars) of imperatoxin-induced substates before and after addition of 40 μM Shaker B. * $p < 0.05$, n=4 paired observations.

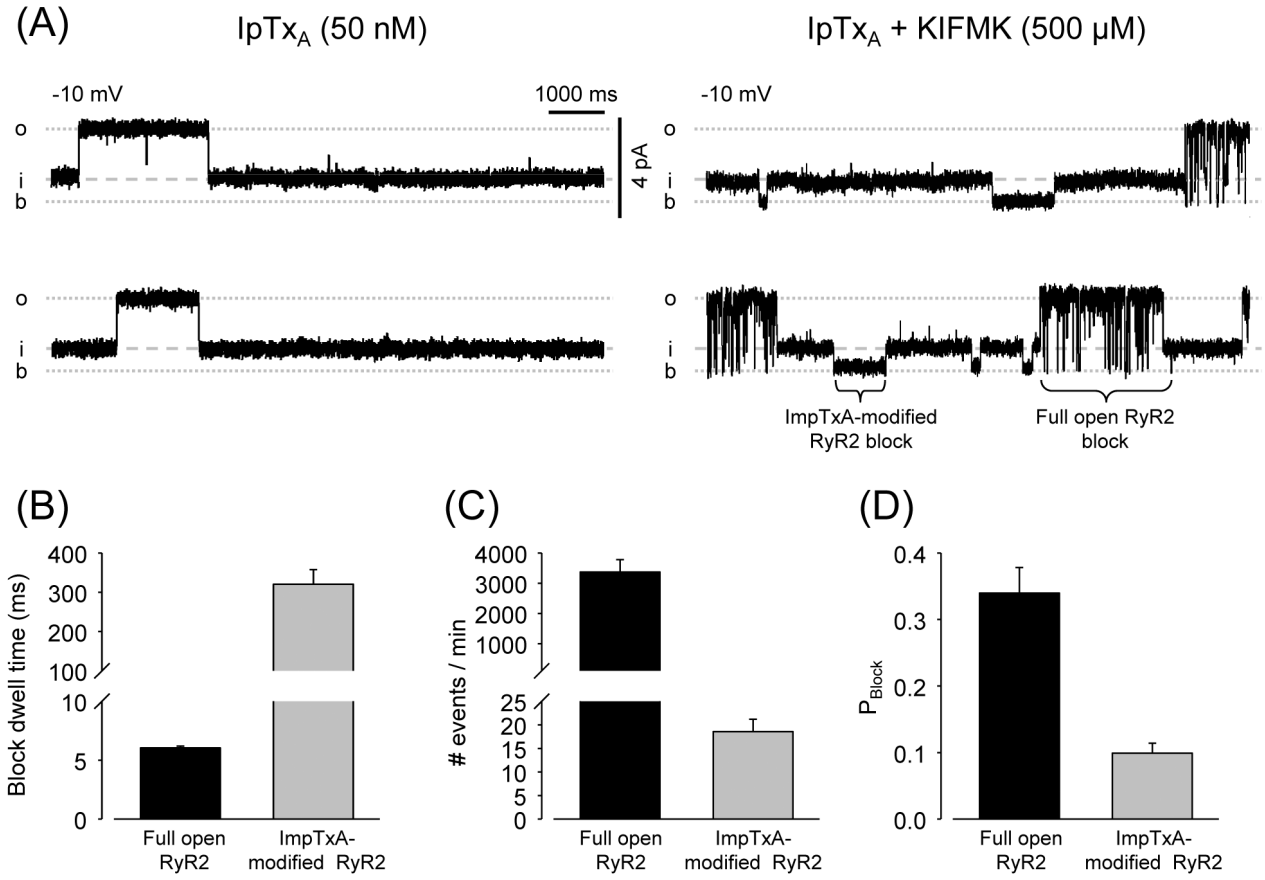

Fig. 5.

Imperatoxin modifies kinetics of RyR2 block by KIFMK. (A) Single-channel recordings of RyR2 with Ca^{2+}/caffeine and IpTx$_A$ (50 nM) at Vm = +10 mV. Traces under control conditions (left) and after addition of 500 μM KIFMK (right) are shown. (B) Dwell times of KIFMK block. (C) Number of block events and (D) Probability of block (P_{block}). Parameters of KIFMK block were estimated during segments of full openings (black bars) and during imperatoxin-induced substates (grey bars). * $p < 0.05$, n=5 paired observations.

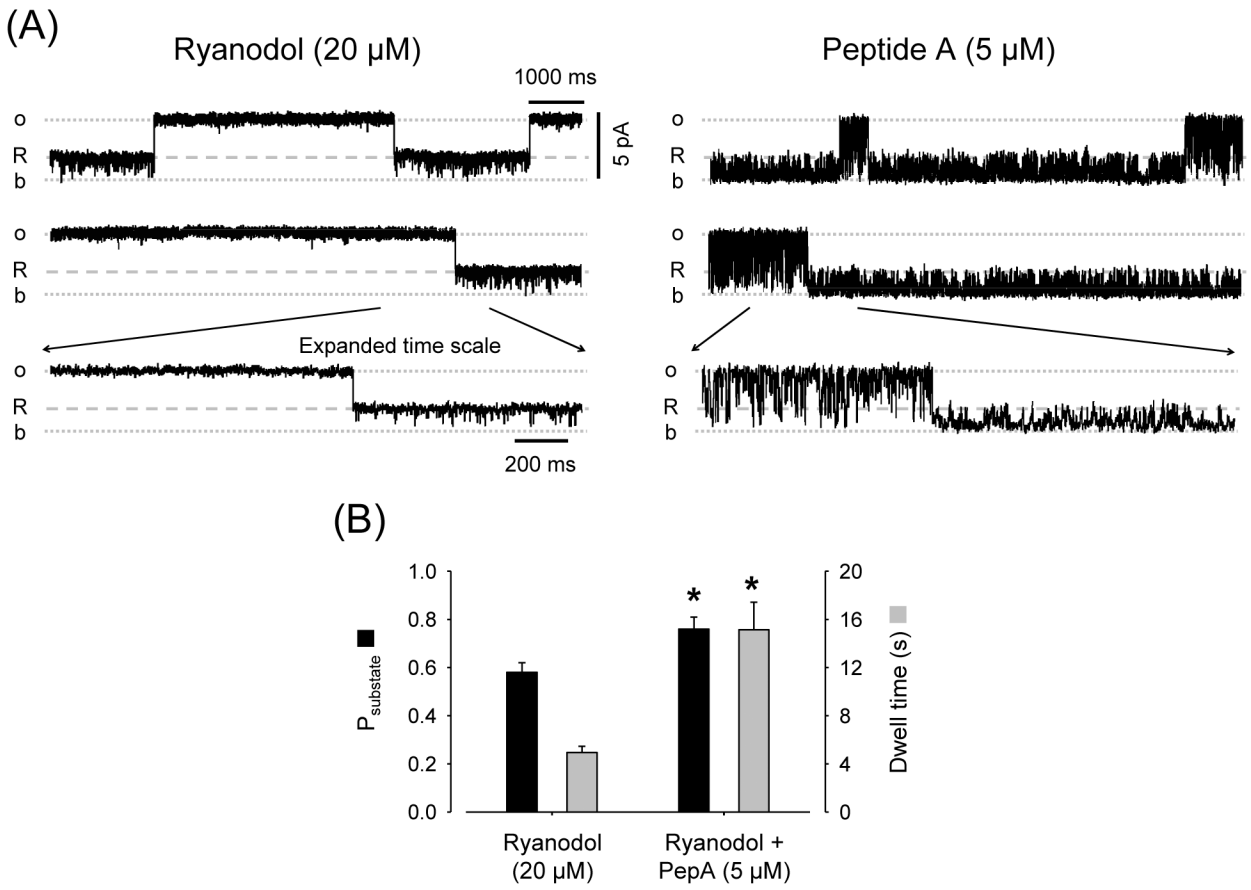

Fig. 6.

Peptide A increases the probability of the Ryanodol substate. (A) Single-channel recordings of a RyR2 in the presence of Ryanodol (20 μM) before and after addition of 5 μM Peptide A (Vm = 0 mV). "R" represents openings to the ryanodol-induced subconductance state. The temporarily expanded traces (lower panels) evidence that Peptide A action is different during full openings vs. ryanodol-induced substates. (B) Probability ($P_{substate}$; black bars) and dwell time (grey bars) of ryanodol-induced substates before and after addition of Peptide A. * $p < 0.05$, n=5 paired observations.

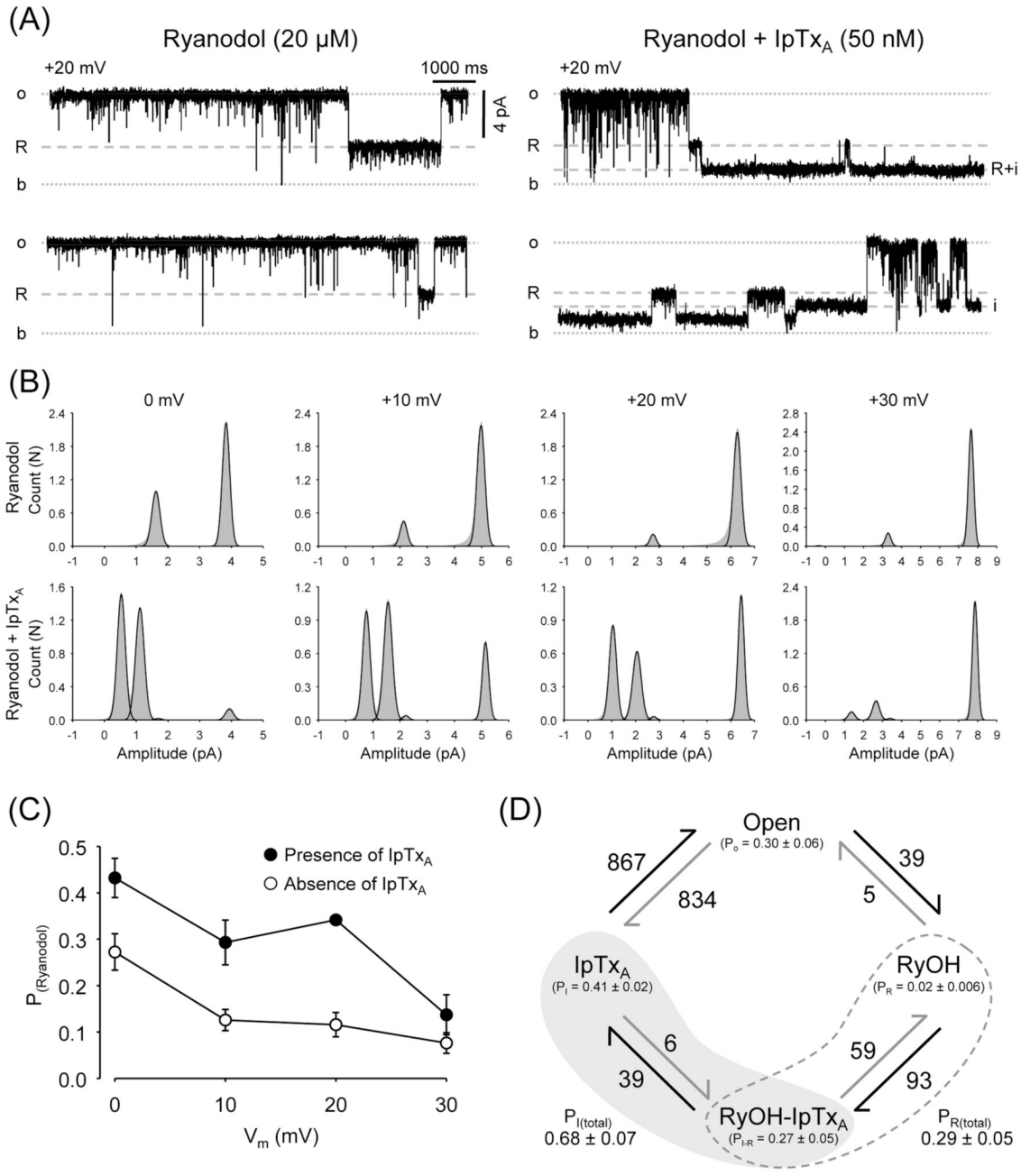

Fig. 7.

Imperatoxin increases the probability of the Ryanodol substate. (A) Single-channel recordings of a ryanodol-modified RyR2 before and after addition of 50 nM IpTx$_A$ (Vm = +20 mV). "R" represents openings to the ryanodol-induced subconductance state. "i" represents opening to the IpTx$_A$-induced substate during RyR2 full openings. "i + R" represents opening to the IpTx$_A$-induced substate when the channel is being modified by ryanodol. (B) Amplitude histograms (grey area) and fits (black lines) at 0, +10, +20 and +30 mV of ryanodol-modified RyR2 before (upper panels) and after addition of 50 nM IpTx$_A$ (lower panels). (C) Probability (P$_{Ryanodol}$) of ryanodol-induced substates before (open circles) and after addition of 50 nM IpTx$_A$ (filled circles) as a function of holding voltage. (D) Diagram of states of RyR2 exposed

to $IpTx_A$ plus ryanodol (40 min recording). The following states were considered: Full openings (Open), $IpTx_A$-induced substate during full openings ($IpTx_A$), Ryanodol modification (RyOH) and $IpTx_A$-induced substate during ryanodol modification (RyOH-$IpTx_A$). State probabilities (P) are given in parenthesis. Arrows represent observed unidirectional transitions from one state to another. Adjacent to each arrow is the respective absolute number of transitions.